

# Universal photocurrent-voltage characteristics of dye sensitized nanocrystalline TiO<sub>2</sub> photoelectrochemical cells

J. S. Agnaldo, J. C. Cressoni, and G. M. Viswanathan

*Laboratório de Energia Solar, Núcleo de Tecnologias e Sistemas Complexos,  
Instituto de Física, Universidade Federal de Alagoas, Maceió-AL, 57072-970, Brazil*

(Dated: October 26, 2018)

We propose a new linearizable model for the nonlinear photocurrent-voltage characteristics of nanocrystalline TiO<sub>2</sub> dye sensitized solar cells based on first principles and report predicted values for fill factors. Upon renormalization diverse experimental photocurrent-voltage data collapse onto a single universal function. These advances allow the estimation of the complete current-voltage curve and the fill factor from any three experimental data points, e.g., the open circuit voltage, the short circuit current and one intermediate measurement. The theoretical underpinning provides insight into the physical mechanisms responsible for the remarkably large fill factors as well as their known dependence on the open circuit voltage.

PACS numbers: 84.60.Jt, 72.80.Le, 05.40.-a, 85.60.-q

## I. INTRODUCTION

An important feature of photovoltaic solar cells and of diverse optoelectronic devices studied in semiconductor physics concerns their current-voltage characteristics [1, 2, 3, 4]. The pioneering work that led to the invention of Grätzel or dye sensitized solar cells became a milestone in the study of photovoltaic devices [5, 6]. Previous theoretical and experimental studies have identified the dependence of the photocurrent and photovoltage on radiant power [7], but not the precise nonlinear dependence of the photocurrent on the photovoltage under conditions of constant radiant power. Moreover, variability in the manufacturing process of dye sensitized solar cells can lead to differences — e.g., variables include the choice of dye, the sintering temperature, thickness of the nanoporous TiO<sub>2</sub> film and choice of chemical treatments. This diversity leads to significant qualitative and quantitative variation in photocurrent-voltage characteristics and of the relevant quantities such as the open circuit voltage  $V_{oc}$  or the fill factor. Such variability has discouraged attempts to identify (possibly “hidden”) dynamical patterns that could yield important insights into the regenerative photoelectrochemical mechanisms that underlie the conversion process. Given the variability and diversity in the characteristics, which properties remain universal and which nonuniversal? More importantly from an experimental point of view, how can we quantitatively model the photocurrent-voltage characteristics, based on fundamental theoretical principles? Here we answer these questions by deriving from first principles an analytical expression for the photocurrent.

The topic of solar energy in general [8, 9, 10, 11] and dye sensitized solar cells in particular [5, 6, 7, 12, 13, 14, 15, 16, 17, 18] attracts broad interest from diverse sectors of society, due to technological, economic, political and environmental considerations. The growing scientific interest in dye sensitized TiO<sub>2</sub> solar cells stems from their unusual features and mode of operation that distinguish them from Si solar cells: (i) efficient charge separation

due to ultra-fast injection of electron from the dye on picosecond and subpicosecond time scales [14, 17]; (ii) conduction consisting only of injected electrons rather than electron-hole pairs [5, 6], due to the wide bandgap of the semiconductor TiO<sub>2</sub>; (iii) high optical density due to the extremely large surface area of the dye sensitized nanoporous semiconductor [14]; (iv) negligible charge recombination with the oxidized sensitizer dye [5, 6, 7]; and (v) very high quantum yields [14]. One important fact that will contribute towards derivation and subsequent interpretation of the current-voltage characteristics concerns how the experimentally measured recombination current density vanishes at short circuit [7] — indicating that the only significant recombination pathway proceeds via back electron transfer into the electrolyte. Indeed, charge recombination between redox species ( $I_3^-$  ions) in the electrolyte and conduction band electrons localized at the nanoporous interface result in suboptimal photovoltage levels — thus limiting the conversion efficiency [19, 20, 21].

## II. METHODS

We begin by assuming that the number of electrons injected into the conduction band depends only on the incident radiant power — in fact the known very high quantum yields justify this assumption. This assumption allows us to express the recombination current density  $J_r$  as a function of the photocurrent density  $J$  and the injection current density. Since  $J_r$  vanishes at short circuit, the injection current equals the short circuit current  $J_{sc}$ , so that

$$J_r = J_{sc} - J . \quad (1)$$

For a well mixed solution with identical surface and bulk concentrations (typical for small current densities), the Butler-Volmer equation [22, 23] leads to the following

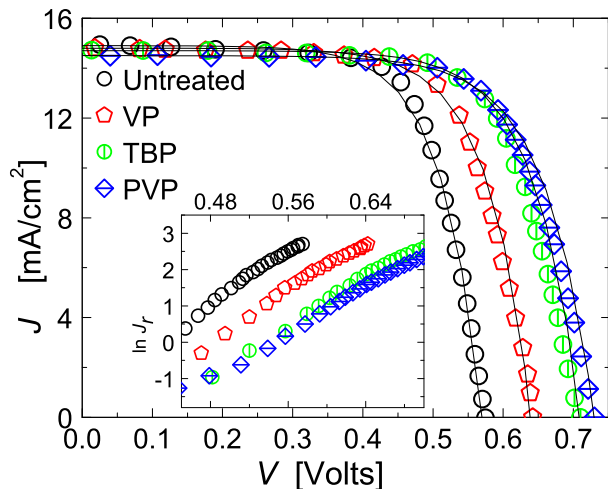


Figure 1: Typical photocurrent voltage characteristics under a radiant power of 1.5 AM for dye sensitized solar cells, taken from ref. [7]. The four data sets have different characteristics due to varied chemical treatments (see text), yet in each case the theoretical curves (solid lines) corresponding to Eq. 6 can account well for the experimental curves. Inset shows approximate logarithmic relation for the recombination current density  $J_r$  versus voltage, not inconsistent with Eq. 3.

expression for the recombination current density  $J_r$ :

$$-J_r = J_0 \left[ \exp(-\alpha_c u f \eta) - \exp(\alpha_A u f \eta) \right], \quad (2)$$

where  $J_0$  denotes the exchange current density,  $u$  the number of electrons transferred in the reaction (and consequently, the order of the rate of reaction for recombination for electrons)  $\alpha_A$  and  $\alpha_C$  the anodic and cathodic transfer coefficients,  $\eta = V$  the overpotential and  $f \equiv q/k_B T$ . With some simplification [7], this equation becomes

$$J_r = q k_{et} c^m n_0^{u\alpha} [\exp(u\alpha q V / k_B T) - 1], \quad (3)$$

where  $\alpha = \alpha_A$  and  $k_{et}$  denotes the back electron transfer rate constant,  $c$  the concentration and  $m$  the order of the reaction for the oxidized species,  $q$  the electronic charge and  $n_0$  represents value in dark conditions of the electron population in the semiconductor.

How do the prefactors depend on voltage  $V$ ? The back electron transfer rate constant varies with radiant power and the maximum, i.e. open circuit, photovoltage  $V_{oc}$ , however we do not expect it to depend on the photovoltage for fixed radiant power. The Nernst Equation for the potential in terms of the concentrations of the oxidized and reduced species holds valid only under equilibrium conditions, yet we know that  $c$  varies across the electrolyte. Indeed, since the reduced species greatly exceeds the oxidized species, we can safely conclude that the voltage varies as  $\Delta V(x) \approx -(k_B T / q) \ln(c^0 / c(x))$ , where  $c(x)$  denotes the concentration at a position  $x$  across the cell (i.e., electrolyte),  $c^0$  denotes a reference

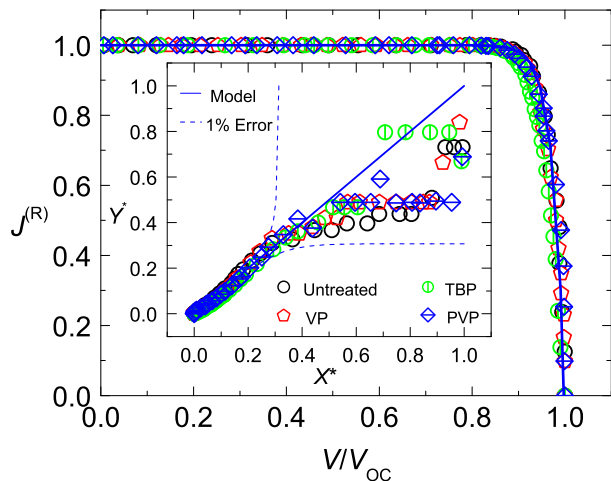


Figure 2: Renormalized photocurrent  $J^{(R)}$  versus  $V/V_{oc}$  for the curves shown in Fig. 1. The data collapse onto a single universal function stable over a variety of chemical treatments and solar cell variability. We have chosen  $v_s = 1/40$ , based on the value of  $k_B T$  at room temperature, for illustration, corresponding to our estimate of an upper bound for fill factors, however we could have renormalized the photocurrent to any fill factor. Indeed, we can linearize the curves, as shown in the inset and explained in the text. The dashed line traces the upper and lower uncertainties corresponding to an error of 1% in the short circuit current. Notice how remarkably the data collapse onto a straight line, within the error tolerance.

(or mean) concentration. Nonetheless, we still do not know, *a priori*, exactly how it varies with the potential at the semiconductor-electrolyte interface as the external load (i.e., impedance) varies, because of the out of equilibrium conditions. In this context, one important clue comes from the dependence on the photovoltage on the electron population. Electrons act as charge carriers in the  $\text{TiO}_2$  — just as the redox species do in the electrolyte. In the semiconductor, injected electrons shift the Fermi level, so that  $n = n_0 \exp(qV/k_B T)$ . This exponential dependence of  $c$  on voltage across the electrolyte, hints at a similar, i.e. exponential, dependence of  $c$  on  $V$  at the interface as the external load varies:

$$V = V_{oc} - (\gamma k_B T / q) \ln(c_{oc} / c). \quad (4)$$

Here  $c_{oc}$  represents the concentration under open circuit conditions and  $\gamma$  represents a free parameter in the model, quantifying the fraction of the voltage variation that affects the oxidized species concentration. Since the triiodide concentration cannot vary very much in the liquid, we cannot expect small  $\gamma$  close to equal unity since this would imply  $c \propto n$ . For now we only mention that one would naïvely expect a positive  $\gamma$  since electron injection and dye regeneration (associated with larger  $V$ ) produce oxidized species.

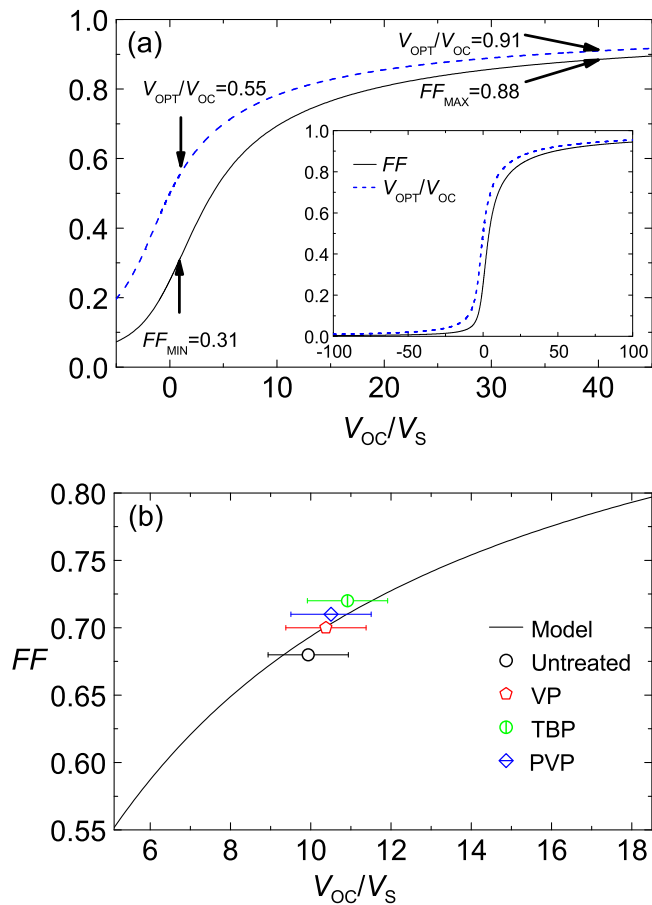


Figure 3: (a) Theoretically predicted fill factors  $FF$  and ratio  $V_{OPT}/V_{OC}$  of optimal operating voltage  $V_{OPT}$  to open circuit voltage  $V_{OC}$  versus  $V_{OC}/V_s$ , where  $V_s$  represents a characteristic voltage (Eq. 7). We estimate a worst-case lower bound on the fill factor using  $V_{OC}/V_s = 1$ , and an idealized upper bound using  $V_{OC}/V_s = 40$ . Inset shows a more complete picture. (b) Comparison of theoretical and experimental values for  $FF$  for the data shown in Fig. 1. Useful real cells will likely have  $FF$  within the range shown.

### III. RESULTS

These considerations immediately lead to an analytical expression for the photocurrent  $J$  as a function of the voltage  $V$  across the cell:

$$J = J_{sc} \left[ 1 - \frac{\exp(mq(V - V_{oc})/\gamma k_B T)}{\exp(u\alpha q V_{oc}/k_B T) - 1} \times \left( \exp(u\alpha q V/k_B T) - 1 \right) \right]. \quad (5)$$

Here  $m \approx 2$  because of the second order reaction and  $u\alpha \approx 0.7$  [7, 13]. This analytical expression must hold true for all dye sensitized solar cells, yet in the context of providing greater clarity and insight we can render it simpler but more useful. Moreover, from a practical point of view, we can simplify it further by making additional yet realistic assumptions. Eq. 3 for the recombination has

validity in the large voltage ( $V > 80\text{mV}$ ) regime [7, 13]. On the other hand, below this potential, the recombination current becomes negligible and uninteresting. For any useful cell,  $n \gg n_0$  by many orders of magnitude, so that we can reasonably well approximate Eq. 5 with

$$J = J_{sc} \left[ \frac{\exp(V_{oc}/V_s) - \exp(V/V_s)}{\exp(V_{oc}/V_s) - 1} \right], \quad (6)$$

where the potential

$$V_s \equiv (k_B T/q) \frac{1}{u\alpha + m/\gamma} \approx \frac{1}{40(0.7 + 2/\gamma)} \text{Volts}, \quad (7)$$

represents a characteristic scale of the exponential decay. Specifically,  $V_s$  quantifies the photovoltage drop corresponding to a decrease in recombination current density by a factor of  $1/e$  where  $e$  here denotes Euler's number. Eqs. 5 and 6 represent the first out of three new results of this article.

Fig. 1 compares the model with photocurrent-voltage curves taken from ref. [7], of untreated and pyridine derivative-treated  $[\text{RuL}_2(\text{NCL})_2]$ -coated nanocrystalline  $\text{TiO}_2$  electrodes in  $\text{CH}_3\text{CN}/\text{MNO}$  (50:50 wt %) containing  $\text{Li}(0.3\text{M})$  and  $\text{I}_2(30\text{mM})$ , for a radiant power of  $100\text{mW}/\text{cm}^2$  (AM 1.5). The electrodes had treatment with following substances: 3-vinylpyridine (VP), 4-*tert*-butylpyridine (TBP), and poly(2-vinylpyridine) (PVP). The good agreement with the data validates the model represented by Eqs. 5 and 6.

The largest possible power output divided by  $J_{sc}V_{oc}$  defines the fill factor  $FF$ . Notice that  $V_s$  changes the fill factor (via  $\gamma$ ). A value  $V_s \rightarrow \infty$  (corresponding to purely resistive or Ohmic behavior) leads to  $FF=1/4$ , whereas  $V_s \rightarrow 0$  leads to unity fill factor — perfect but theoretically impossible except at  $T = 0$  K. Most dye sensitized solar cells have  $FF=0.6-0.7$  (Fig. 1).

We now turn our attention to the question of whether a single universal current-voltage relation can describe all  $\text{TiO}_2$  solar cells. According to the theory presented above, all dye sensitized solar cells must satisfy Eq. 5 if not Eq. 6. If we renormalize the photovoltage to obtain an adimensional measure  $V^* \equiv V/V_{oc}$ , then every single dye sensitized solar cell must satisfy the following relation for an idealized renormalized photocurrent:

$$J^{(R)} \equiv \frac{1 - \left[ 1 - (J/J_{sc}) \left( 1 - \exp(-V_{oc}/V_s) \right) \right]^{V_s/V_{oc}v_s}}{1 - \exp(-1/v_s)}. \quad (8)$$

Here  $v_s$  fixes the shape or fill factor of the renormalized photocurrent. Fig. 2 shows the predicted data collapse. We have chosen a value  $v_s = 1/40$ , due to its significance for an idealized solar cell with maximum  $FF$  (see below) at room temperature. However, we can obtain data collapse for any  $v_s$  (not shown). This is perhaps more clear if we linearize the curves. We define coordinates

$$X^* \equiv 1 - V/V_{oc} \quad (9)$$

$$Y^* \equiv -V_s/V_{oc} \ln \left[ 1 - \frac{J}{J_{sc}} \left( 1 - \exp(-V_{oc}/V_s) \right) \right] \quad (10)$$

The inset of Fig. 2 shows how the data collapse onto a straight line. All dye sensitized solar cells thus follow the same universal pattern of photocurrent-voltage behavior.

We next consider the problem from the point of view of scale invariance symmetry. The fill factor cannot depend on  $J_{sc}$ , since it cancels in the power ratio. It also remains invariant under a scale transformation  $V_{oc} \rightarrow \lambda V_{oc}$ ,  $V_s \rightarrow \lambda V_s$ . In fact, no dilation can alter a ratio of geometric areas. The invariance of FF for arbitrary  $\lambda$  implies that FF can depend on  $V_{oc}$  and  $V_s$  only via their ratio:

$$FF = FF(V_{oc}/V_s) . \quad (11)$$

The exact functional dependence appears to involve a transcendental equation. We are still attempting an analytical solution using the Lambert W function. Nevertheless, it is susceptible to numerical solution. Fig. 3(a) shows FF as a function of  $V_{oc}/V_s$ .

We next comment on the values typically found for  $V_s$  and their physical significance. The values found correspond to negative  $\gamma$  and thus suggest that the concentration of redox species ( $I_3^-$  ions) decreases with the photovoltage. This may at first seem counter-intuitive. Indeed, higher voltage suggests larger electron population and more injection. Moreover, the regeneration of the dye creates  $I_3^-$  species, in the proportion of one ion for every two electrons injected.

So do we face an apparent inconsistency? The important fact, mentioned earlier, of zero recombination current density  $J_r = 0$  under short circuit conditions, hints at the correct explanation: the rate of regeneration of the oxidized dye depends not on the photovoltage (zero under short circuit) but rather on the rate of electron injection — thus only on the open circuit photovoltage, or alternatively, on the radiant power. The finding agrees with the expectation of a smaller depletion layer for more external current drain.

The above findings allow us to estimate lower and upper limits for FF. Purely Ohmic behavior corresponds to  $V_s \rightarrow \infty$  and  $FF=1/4$ , however we cannot imagine this scenario. For any useful device, the largest conceivable value of  $V_s$  should not exceed  $V_{oc}$ , which gives us a lower bound for FF of  $FF=0.31$  and an optimal operational voltage of  $V_{OPT} = 0.55 V_{oc}$ . By considering  $V_s = 1/40$  Volts, i.e. idealizing  $u\alpha = 1$ ,  $m/\gamma = 0$ , and  $V_{oc} = 1$ , we arrive at an upper bound of  $FF=0.88$  and  $V_{OPT} = 0.91 V_{oc}$ , as shown in Fig. 3(a). For  $u\alpha = 0.7$  we obtain slightly smaller FF. Fig. 3(b) allows one to estimate one among  $V_s$ ,  $V_{oc}$  and  $FF$  from the other two

and will thus find practical application. We estimated the error bars for the experimental points from the regression fits used to arrive at the values of  $V_s$ . Devices that we constructed locally had values of FF within these bounds.

Finally, our findings explain the very large fill factors of dye solar cells. The recombination current becomes insignificant as soon as the voltage drops to  $V = V_{oc} - V_s$  (Eqs. 3, 6). If  $V_s \ll V_{oc}$  (as in fact happens), then the photocurrent jumps from zero to close to its short circuit value even if the voltage only drops slightly (i.e., by  $V_s$ ). Notice from Fig. 3 that increases in  $V_{oc}$  — e.g., due to greater radiant power — should indeed lead to higher FF if  $V_s$  varies much less than  $V_{oc}$ , as in fact occurs.

#### IV. DISCUSSION AND CONCLUSION

We briefly comment on conversion efficiency. Since we cannot expect to change  $V_s$  significantly, further increases in efficiency will depend mainly on increasing the open circuit photovoltage, which in turn also requires reducing losses due to charge recombination at the nanoporous interface — the main challenge indeed. Moreover, we know that  $c \sim n^{1/\gamma}$ , where  $\gamma$  has the negative value  $\gamma \approx -6$ . In other words, we find evidence of a fractional power law or scaling exponent, indicating self-affine behavior. We hypothesize that the negative value arises due to the fact that larger  $n$  leads to greater recombination, which consumes the oxidized species. Localization effects and transport properties play an important role in this context [18].

In summary, our theoretical results appear to account well for the observed behavior of real dye sensitized solar cells and seem to provide new insights into their functioning. Among the important results reported here, we note that Fig. 3 allows one to calculate FF knowing  $V_{oc}/V_s$  or vice versa. Moreover, knowing either one or the other, one can readily obtain the entire photocurrent-voltage curve, via Eq. 6. From just 3 points in the photocurrent-voltage curve, one can reconstruct the entire curve. The findings reported here may thus allow further advances and eventually lead to technological innovations.

We thank BNB, CAPES and CNPq for research funding and I. M. Gléria, A. S. Gonçalves, M. L. Lyra, M. R. Meneghetti, S. M. P. Meneghetti, F. A. B. F. de Moura, A. F. Nogueira and L. S. Roman, E. C. Silva for discussion. GMV thanks S. B. Manamohan for discussions in 1989.

- 
- [1] S. M. Sze, *Physics of Semiconductor Devices* (J. Wiley & Sons, New York, 1981).  
 [2] D. A. Fraser, *The Physics of Semiconductor Devices* (Clarendon Press, Oxford, 1990).  
 [3] G. Burns *Solid State Physics* (Academic Press Inc. New

- York, 1985).  
 [4] H. J. Snaith and M. Grätzel, *Applied Phys. Lett.* **89**, 262114 (2006).  
 [5] B. O' Regan, M. Grätzel, *Nature (London)* **53**, 737 (1991).

- [6] M. Grätzel, *Nature (London)* **414**, 338 (2001).
- [7] S. Y. Huang, G. Schlichthörl, A. J. Nozik, M. Grätzel, and A. J. Frank, *J. Phys. Chem. B* **101**, 2576 (1997).
- [8] M. Grätzel, J. -E. Moser, *Solar Energy Conversion, Electron Transfer in Chemistry* **5**, 589, eds V. Balzani and I. R. Gould (Wiley-VCH, New York, 2001).
- [9] W. A. Gazotti, A. F. Nogueira, E. M. Girotto, M. C. Galazzi, M. A. Paoli, *Synthetic Metals* **108**, 151 (2000).
- [10] A. F. Nogueira, J. R. Durrant, M. A. Paoli, *Advanced Materials* **13**, 826 (2001).
- [11] L. S. Roman, M. Berggren, O. Inganäs, *App. Phys. Lett.* **75**, 3557 (1999).
- [12] H. J. Snaith, L. Schmidt-Mende, and M. Grätzel, *Phys. Rev. B* **74**, 045306 (2006).
- [13] S. K. Deb, S. Ferrere, A. J. Frank, B. A. Gregg, S. Y. Huang, A. J. Nozik, Z. Schlichthörl, and A. Zaban, *Conf. Rec. IEEE Photovoltaic Spec. Conf.* **26**, 507 (1997).
- [14] J. R. Durrant, J. Nelson, D. R. Klug, *Materials Science and Technology* **16**, 1345 (2000).
- [15] N. Kopidakis, K. D. Benkstein, J. Lagemaat, A. J. Frank, Q. Yuan and E. A. Schiff, *Phys. Rev. B* **73**, 045326 (2006).
- [16] J. van de Lagemaat, N. Kopidakis, N. R. Neale, and A. J. Frank, *Phys. Rev. B* **71**, 035304 (2005).
- [17] N. J. Cherepy, G. P. Smestad, M. Grätzel, and J. Z. Zhang, *J. Phys. Chem. B* **101**, 9342 (1997).
- [18] J. Nelson, *Phys. Rev. B* **59**, 15374 (1999).
- [19] A. Stanley and D. Matthews, *Aust. J. Chem.* **48**, 1924 (1995).
- [20] G. Smestad, *Sol. Energy Mater. Sol. Cells* **32**, 273 (1994).
- [21] P. Liska, Ph. D. Thesis of Swiss Federal Institute of Technology (1994).
- [22] A. J. Bard, L. R. Faulkner *Electrochemical Methods* (J. Wiley & Sons, New York, 1980).
- [23] A. Więckowski, *Interfacial Electrochemistry: Theory, Experiment, and Applications*, (CRC Press, 1999).